

RESEARCH ARTICLE

10.1029/2017JG004082

Key Points:

- *Tridacna maxima* in Okinotori Island made daily growth increments, and increment-based chronology provided dates for geochemical analysis data
- $\delta^{18}\text{O}_{\text{shell}}$ reflected annual SST fluctuations in Okinotori Island
- The decrease in increment thickness and positive peaks in the shell Ba/Ca ratio and $\delta^{18}\text{O}_{\text{shell}}$ corresponded to fall season typhoon approaches to the island

Supporting Information:

- Supporting Information S1
- Figure S1
- Figure S2

Correspondence to:

T. Watanabe,
 wabe@sci.hokudai.ac.jp

Citation:

Komagoe, T., Watanabe, T., Shirai, K., Yamazaki, A., & Uematu, M. (2018). Geochemical and microstructural signals in giant clam *Tridacna maxima* recorded typhoon events at Okinotori Island, Japan. *Journal of Geophysical Research: Biogeosciences*, 123, 1460–1474. <https://doi.org/10.1029/2017JG004082>

Received 4 AUG 2017

Accepted 6 APR 2018

Accepted article online 19 APR 2018

Published online 7 MAY 2018

Corrected 15 JUN 2018 and 6 JUL 2018

This article was corrected on 15 JUN 2018 and 6 JUL 2018.

Geochemical and Microstructural Signals in Giant Clam *Tridacna maxima* Recorded Typhoon Events at Okinotori Island, Japan

Taro Komagoe^{1,2} , Tsuyoshi Watanabe^{1,2} , Kotaro Shirai³ , Atsuko Yamazaki^{1,2,4} , and Mitsuo Uematu³ 

¹Department of Natural History Sciences, Faculty of Science, Hokkaido University, Sapporo, Japan, ²KIKAI institute for Coral Reef Sciences, Kikai town, Japan, ³Atmosphere and Ocean Research Institute, The University of Tokyo, Kashiwa, Japan,

⁴Department of Earth and Planetary Sciences, Faculty of Science, Kyushu University, Fukuoka, Japan

Abstract To validate the usability of the giant clam shell as a recorder of short-term environmental changes such as typhoons, we collected a live *Tridacna maxima* from Okinotori Island, Japan, on 15 June 2006. Growth increment thickness, stable isotope ratio ($\delta^{18}\text{O}_{\text{shell}}$, $\delta^{13}\text{C}_{\text{shell}}$), and the barium/calcium ratio (Ba/Ca) in the *T. maxima* shell sample were measured and compared to Okinotori Island instrumental environmental data. In the outer layer of the shell sample, there were 365 ± 6 growth increments per year, as estimated by the $\delta^{18}\text{O}_{\text{shell}}$ profile compared with sea surface temperature. The growth increments in the specimen were formed daily, and thus, we can determine the date of the sampling points of $\delta^{18}\text{O}_{\text{shell}}$, $\delta^{13}\text{C}_{\text{shell}}$ and the Ba/Ca ratio by counting growth increments. After typhoon approach, there is a decrease in increment thickness and some disturbed growth increments. The positive peaks in the shell Ba/Ca ratio and $\delta^{18}\text{O}_{\text{shell}}$ corresponded to lower sea surface temperature caused by typhoons. These results indicated that the microstructural and geochemical record in *Tridacna maxima* shells could be useful for detecting past typhoon events.

1. Introduction

In recent years, with global warming of the climate, there is concern that the frequency of major tropical cyclones such as typhoons, hurricanes, or cyclones will increase (IPCC, 2013). The passage of major tropical cyclones is a weather phenomenon that occurs in a few days but sometimes causes great damage to human society. Clarifying the frequency of tropical cyclones in an era warmer than the present age would provide important information for predicting the frequency of tropical cyclones caused by global warming. Paleotempestology has sought to develop tropical cyclone activities over a large range of time scales, from daily to millennial-scale reconstructions (Muller et al., 2017). The more commonly used archives for past tropical cyclone activities include (1) historical documentary record, such as official histories, gazettes, newspaper, and civilian writings like travel logbooks, diaries, and poems (Fan & Liu, 2008); (2) speleothem (Frappier, 2008; Haig et al., 2014), coral-ring (Hetzinger et al., 2008; Kilbourne et al., 2011), tree ring archives (Miller et al., 2006; Li et al., 2011; Knapp et al., 2016; Trouet, Harley, & Domínguez-Delmás, 2016), and ostracoda (Lane et al., 2017; Lawrence et al., 2008); (3) beach ridges (Forsyth et al., 2010; Nott, 2011; Nott et al., 2009; Nott & Forsyth, 2012); and (4) coastal lacustrine, lagoonal, and marsh overwash deposits (Horton et al., 2009; Williams, 2012; Woodruff et al., 2009). However, there are no daily records before human history in historical documents, and it is difficult to clarify individual typhoons due to the insufficient time resolution of these past tropical cyclone archives. Therefore, a proxy to clarify the occurrence of typhoons with high temporal resolution is important for high-resolution paleotempestology applications.

The giant clam (Tridacnidae) is widely distributed over the coral reefs in Indo-Pacific oceans and forms the largest shells among all bivalves (Rosewater, 1965). Symbiotic algae (zooxanthellae) in their hypertrophied mantle enable rapid growth, for example, approximately 15 mm/yr in a *Tridacna gigas* inner shell layer (Watanabe et al., 2004). Annual and daily growth increments were recognizable in the shells of *T. gigas*, *Tridacna maxima*, *Tridacna squamosa*, and *Hippopus hippopus* (Aharon & Chappell, 1986; Aubert et al., 2009; Bonham, 1965; Duprey et al., 2014; Pannella & MacClintock, 1968; Pätzold et al., 1991; Sano et al., 2012; Warter et al., 2015; Watanabe et al., 2004; Watanabe & Oba, 1999). Counting daily growth increments provides us exact deposition dates for daily increments. This attribute also allows precise dating for geochemical analysis data

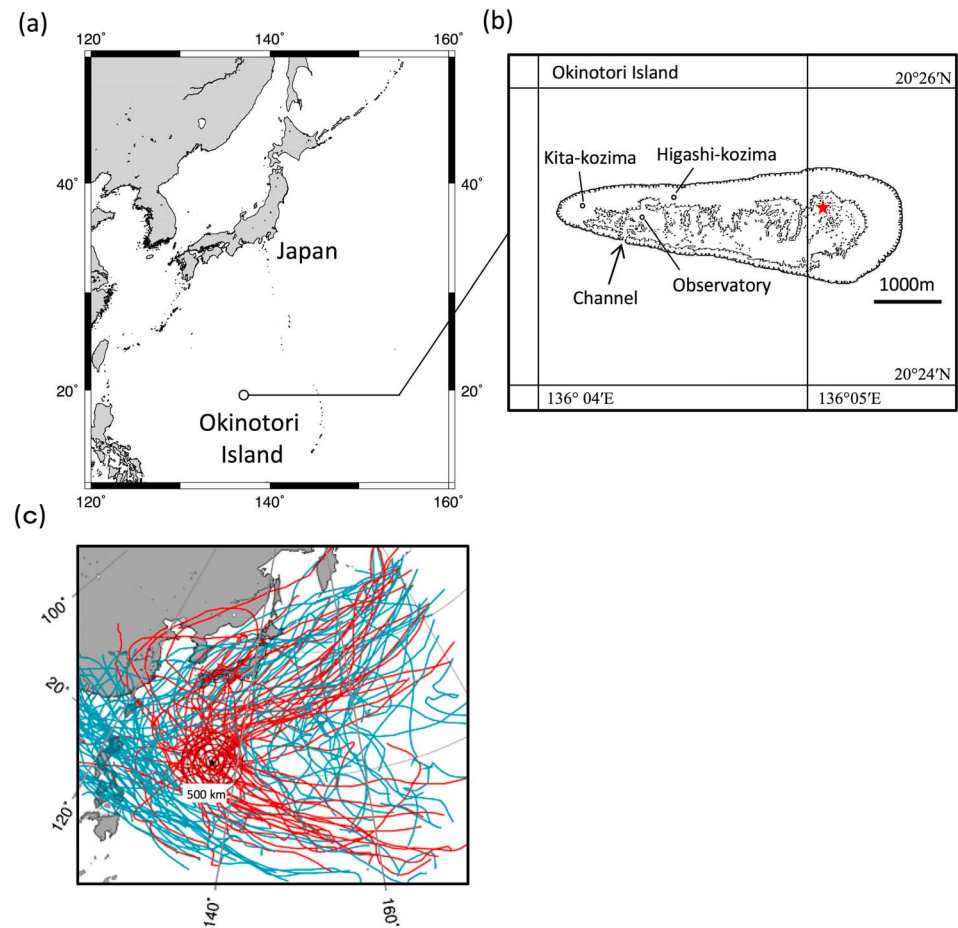


Figure 1. (a) Location of Okinotori Island (black circle; 20°25'N, 136°05'E), (b) Okinotori (20°25'N, 136°05'E) and sampling point (star), and (c) trajectory of typhoons 1993–1998 (modified from Iwao et al., 2002). Okinotori Island locates passage of typhoons approach Japan. Forty-six (red) of 157 (blue) typhoons passed in radius of 500 km from Okinotori Island.

from a *Tridacna* shell (Aubert et al., 2009; Duprey et al., 2014; Watanabe & Oba, 1999). Growth pattern analysis is useful for reconstruction of past environments with daily resolution (upwelling: Aubert et al., 2009; Cyclone: Schwartzmann et al., 2011). In addition, *Tridacnidae* precipitates a dense aragonite shell resistant to diagenetic alteration. Growth increments are well preserved in a fossil shell specimen and give accurate paleoenvironmental records (Aharon & Chappell, 1986; Ayling et al., 2015; Komagoe et al., 2016; Warter et al., 2015; Watanabe et al., 2004; Warter & Müller, 2017).

The oxygen-stable isotope ratios ($\delta^{18}\text{O}$) of a biogenic carbonate-including bivalve shell are a function of both sea surface temperature (SST) and the oxygen isotopic composition of the surrounding seawater ($\delta^{18}\text{O}_{\text{sw}}$; Epstein et al., 1953; Grossman & Ku, 1986). The $\delta^{18}\text{O}$ of biogenic carbonates sometimes deflects from the isotopic equilibrium with surrounding seawater; this is called the “vital effect” (Horibe & Oba, 1972; Urey et al., 1951, e.g., coral skeleton). However, *Tridacna* shells calcify essentially in isotopic equilibrium with surrounding seawater (e.g., Aharon, 1983; Watanabe & Oba, 1999). $\delta^{18}\text{O}$ of bivalve shell ($\delta^{18}\text{O}_{\text{shell}}$) is sometimes affected by ontogenetic growth (e.g., Goodwin et al., 2003). However, *Tridacna* shell has a fast growth rate and large daily growth increment. Therefore, *Tridacna* $\delta^{18}\text{O}_{\text{shell}}$ provides high-resolution paleotemperature reconstruction on decadal to century time scales (Watanabe & Oba, 1999). In addition, previous studies have suggested that *Tridacnidae* shell is secreted in isotopic equilibrium with seawater (Aharon, 1991; Aharon & Chappell, 1986; Duprey et al., 2014; Jones et al., 1986; Romanek & Grossman, 1989; Watanabe & Oba, 1999). The earlier study of Romanek and Grossman (1989) revealed that the $\delta^{18}\text{O}_{\text{shell}}$ profile of the giant clam *T. maxima* recorded seasonal SST periods. *T. maxima* has the widest distribution in the Indo-Pacific Ocean in

Tridacnidae (Moir, 1986) and generally occurs in geological and archeological fossil assemblages (Faylona et al., 2011).

Barium has a nutrient-like distribution in the ocean, and the coralline barium/calcium ratio (Ba/Ca) has been used as record of upwelling events in the tropical ocean (Lea et al., 1989). In bivalve species, common mussel (*Mytilus edulis*) calcite shell Ba/Ca profiles appear to show seasonal peaks in Ba associated with changes in particulate Ba, dissolved Ba, or phytoplankton productivity (Gillikin et al., 2006). Similarly, Ba/Ca peaks in the inner shell layer of *T. gigas* appear to reflect the timing and amplitude of chlorophyll peaks associated with phytoplankton blooms (Elliot et al., 2009).

In this study, we measured growth increment width, $\delta^{18}\text{O}_{\text{shell}}$, and Ba/Ca in *T. maxima* from Okinotori Island, a site in the open ocean in the tropical western Pacific. Okinotori Island is very isolated from any sources of anthropogenic contamination, and the island is in the path of typhoons approaching Japan (Figure 1). From 1993 to 1998, 46 of 157 typhoons passed within a radius of 500 km from the island (JAMSTEC). According to Japan Meteorological Agency's classification of typhoon zone, 500 to 800-km radius typhoon is called major typhoon and there is possibility of blowing wind speed of 15 m/s or more. *T. maxima* from Okinotori Island is thus appropriate for an investigation of whether the giant clam can be used as a record of abrupt environment changes. The aim of this study was to validate whether the shell of *T. maxima* in Okinotori Island, Japan, could record daily- to weekly-scale environmental events such as typhoons.

2. Materials and Methods

2.1. Okinotori Island and *Tridacna maxima* Sample

Okinotori Island (20°25'N, 136°05'E) is the southernmost island (an atoll) in Japan and is isolated from islands with human inhabitants (Figure 1). Thus, there are few terrestrial and artificial effects on its coral reefs. According to general seasonal SST variation for Okinotori Island (statistics processed for April 1993 to February 2001) reported in Nakano et al. (2001), SST in Okinotori Island monotonously rises through April to June and reaches up to 29.5 °C in July. SST in Okinotori Island exceeds 29 °C from June to September. After that, SST decreases gradually from October to February. The average amplitude of annual SST changes in Okinotori Island is 4.8 °C (Nakano et al., 2001). A living *Tridacna maxima* specimen was collected at 2 m depth in the coral reef of Okinotori Island on 15 June 2006, during the cruise KH-06-2 of the Research Vessel (R/V) *Hakuhoumaru*. We caught few *Tridacna maxima* specimen from the island, and we used the youngest shell specimen with fast growth rate to detect the geochemical and sclerochronological signals during typhoon approaches. The shell was 12.8 cm long and 8.6 cm tall (umbo-edge; Figure 2a). All *Tridacnidae* in Okinotori Island are *T. maxima* (Yoneyama et al., 2006).

2.2. Sample Preparation

The soft tissues of the *T. maxima* specimen were removed immediately after collection. The shell was put into a polyester solidifier (p-resin, Geoscience Materials Nichika) to prevent breakage of the shell outer layer structure during cutting. The shell was cut in two 10-mm-thick sections with a stonecutter (blade thickness 0.5 mm), along the maximum growth axis (Figures 2a and 2b). One shell section was for geochemical analysis, and the other was for sclerochronological analysis (Figures 2b–2d). The sections were polished with #800, #2000, and #8000 polishing powder. The sections were ultrasonically rinsed (ultrasonic bath, SND corp. US-207) in deionized water for 15 min between the three rounds of polishing.

2.3. Sclerochronological Methodology

To emphasize the growth increments, one shell section was immersed in Mutvei's solution (Schone et al., 2005). Increments were clearly observed after 15 min of etching in Mutvei's solution (500-mL acetic acid 1%, 500-mL glutaraldehyde 25%, and 0.1 g of alcian blue powder) at 37–40 °C (Figure 2d). Photographs of the shell section were taken under a digital microscope (KEYENCE VHX-2000), and the increment thickness in the outer layer was measured using the image processing software ImageJ (Rasband, W.S., 1997–2015). The increments were measured in the recent (edge; collected date) to old direction along the growth axis, corresponding to the geochemical analysis transect on the other section (Figure 2d). By comparing composite photographs of geochemical and sclerochronological analysis shell sections, we can determine the calendar date for the geochemical analysis results.

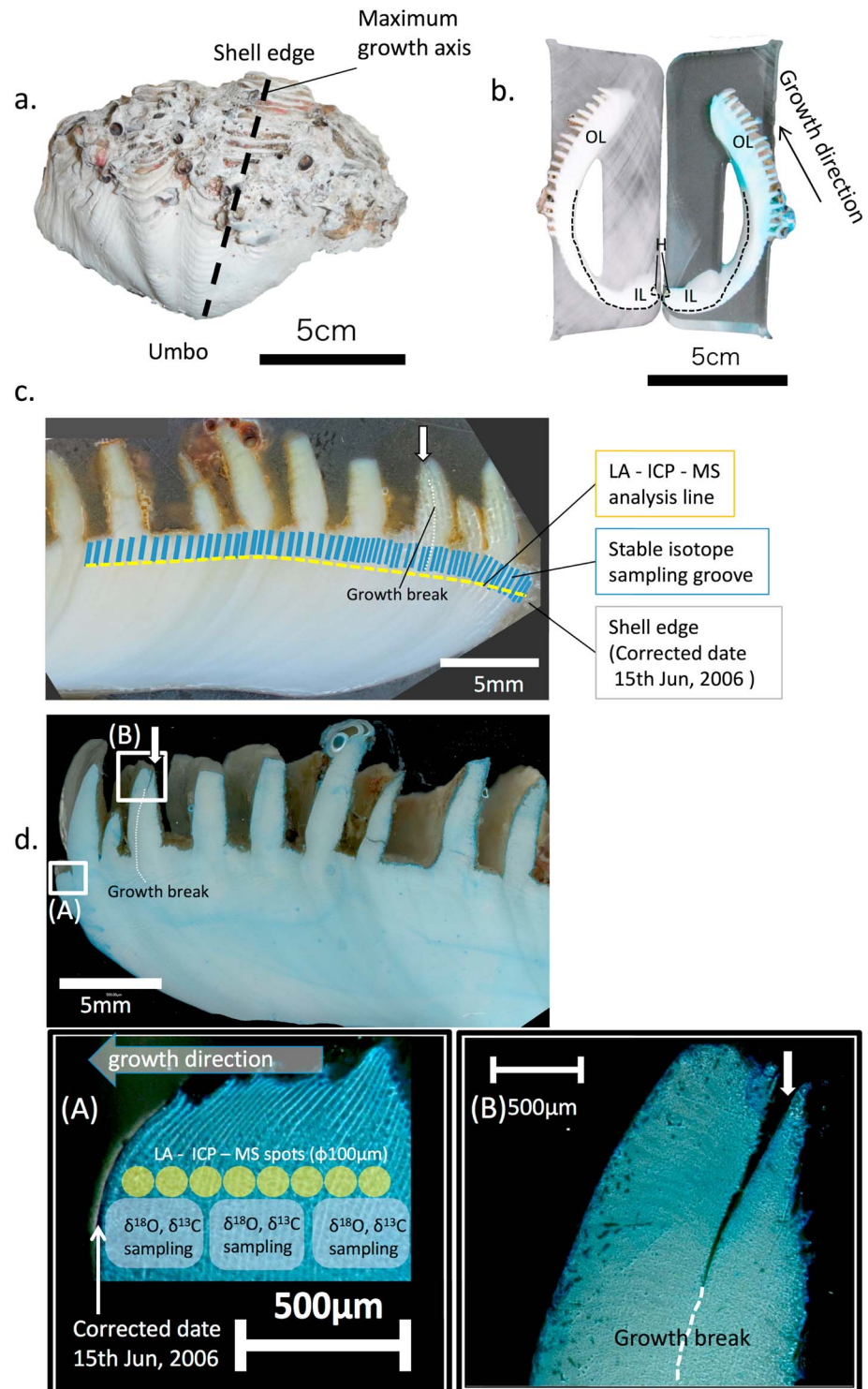


Figure 2. The shell samples of *Tridacna maxima* specimen. (a) The whole *Tridacna maxima* valve. The dotted line shows maximum growth axis. (b) Thick shell sections from maximum growth axis. The left one is for geochemical analysis, and the right one is for sclerochronological analysis, outer layer (OL), inner layer (IL), and hinge area (H). (c) Sampling design for geochemical analysis and (d) microscopic image of the shell microgrowth lines. (A) Enlarged image of the shell edge and shows sampling design for geochemical analysis in another shell section and (B) enlarged image of the growth break in the shell ornamentation. The growth break continued to sampling line.

2.4. Stable Isotope Analysis

Powder samples for isotope analysis were taken from the pair of shell sections (Figure 2c). Each sample was obtained from the parallel to the growth increments using a hand drill (HP-200S, Toyo associates Co., Ltd., Japan) with a 0.4-mm drill bit (model BS1201, Minitor Co. Ltd., Japan; Figure 2d). The sampling grooves were taken discretely and constantly had an average length of 400 μm , depth of 500 μm , and width of 400 μm of providing around 200- μg powder samples for isotope analysis. Each sampling groove contained 8–36 increments depending on shell growth rates (Figure 2c). The 20- to 40- μg powder samples were reacted with 100% phosphoric acid at 70 $^{\circ}\text{C}$ in a carbonate preparation device (Kiel IV Carbonate preparation device), and the produced CO_2 was analyzed using a stable isotope ratio mass spectrometer (Thermo Scientific MAT 253). Isotopic values ($\delta^{18}\text{O}$ and $\delta^{13}\text{C}$) were one-point calibrated against National Bureau of Standards (NBS) 19 and reported in standard δ notation relative to Vienna Pee Dee belemnite and confirmed the calibration using NBS 18. The standard deviations (1σ) for 22 replicate measurements of NBS 19 are 0.03‰ and 0.02‰ for $\delta^{18}\text{O}$ and $\delta^{13}\text{C}$ as external long-term reproducibility throughout this study, respectively.

2.5. Analysis of the Barium/Calcium Ratio

Barium and calcium concentrations were analyzed by Laser Ablation Inductively Coupled Plasma Mass Spectrometry (Agilent 7700 ICP-MS coupled with New Wave Research NWR193 laser ablation system: 193-nm ArF excimer laser [pulse width < 5 ns]) along the same sampling line used for isotopic analysis sampling (Figure 2c). The laser conditions were as follows: irradiance 0.82 GW/cm^2 , repetition rate 10 Hz, and 40 s of laser duration. The sample surface was cleaned by 5 s of preablation. The shell sample was ablated using a 100- μm laser spot, and each spot was adjacent to its neighbor, without overlap. There were 2 to 6 growth increments in each ablated spot. The calibration of the signal intensity to the Ba/Ca ratio was performed using glass standard materials: NIST 612 standard glass distributed by the National Institute of Standard and Technology (Shirai et al., 2008). ^{43}Ca was used as an internal standard, and ^{138}Ba was expressed in terms of its molar ratio to ^{43}Ca . The analytical error for the Ba/Ca ratio (relative standard deviation) was within 3.86% ($n = 42$, 1σ NIST612) as external long-term reproducibility throughout this study. After isotopic and Ba/Ca ratio analysis, the sampling grooves and spots on the shell section were compared to the growth increment positions by overlaying photographs of the sections.

2.6. Environmental Data

The SST in Okinotori Island was observed by the Japan Agency for Marine-Earth Science and Technology (JAMSTEC; SST data available at the JAMSTEC Okinotori Island Web site, <http://www.jamstec.go.jp/j/database/okinotori/index.html>). The SST was measured in 40-min intervals at an automatic observatory in Okinotori Island. These data sets were converted into daily averages to compare to the temporal resolution of the isotope analysis. The data on temporal chlorophyll *a* concentrations (8-day binned data available at NASA's Ocean Color Web, <http://oceancolor.gsfc.nasa.gov/>) were obtained from a 9 km \times 9 km pixel containing Okinotori Island in Sea-viewing Wide Field-of-view Sensor (McClain et al., 2004) by Yamazaki et al. (2011). The outgoing longwave radiation (OLR) is the intensity of infrared emission from ocean, land, or cloud surfaces, which decreases with cloud cover. Cloud surfaces emit relatively shortwave radiation, reflecting the cooling temperature altitude. In contrast, warming surfaces emit longwave radiation. In the tropical zone, low OLR values show active convective activity and much rainfall. OLR can be used as an indicator of high sunlight-like OLR in strong sunlight (Shupe & Intrieri, 2004). Typhoons that passed over Okinotori Island were defined from the past position of typhoons in a weather chart (Japan Meteorological Agency), and the wind speed at Okinotori Island was observed by JAMSTEC (wind speed data available at <http://www.jamstec.go.jp/j/database/okinotori/index.html>).

3. Results

3.1. Sclerochronological Record and Chronology for *T. maxima*

The growth increments in the shell section appeared under microscopic observation as a pair of less-etched white lines (growth lines) and deeply etched blue bands (growth increments) when stained with Mutvei's solution (Figure 2d). There were 937 increments observed in the shell section (five-time replication

counting error was within $\pm 1.3\%$ of increments number). The thicknesses of the increments ranged from 6.16 to 59.9 μm , and the average thickness was 25.2 μm . Bivalves sometimes form irregular growth increment patterns called “growth breaks” (Kennish & Olsson, 1975). There is a distinct growth break characterized by a deep V-shaped notch in the outer shell layer at the 230th growth increment counted from the shell edge and the growth break continued to the measurement part (Figures 2c and 2d). In addition, there are growth breaks in which width suddenly decreased appearing at the 98th, 122nd, 241st, 411th, 617th, 795th, 831st, and 858th growth increments (Figure 3, arrow marks).

To assign calendar dates to the isotope ratios and Ba/Ca ratio, the age model was established using the number of growth increments (Figure 3). The growth increments in *T. maxima* shells are formed daily; that is, they are a “daily growth increment” (Duprey et al., 2014). We determined the date of sampling spots for $\delta^{18}\text{O}$, $\delta^{13}\text{C}$, and the Ba/Ca ratio by counting growth increments from the shell edge (collected on 15 June 2006) toward each center of sampling spot (Figure 3). The shell $\delta^{18}\text{O}$ minima were at the 108th, 455th, and 886th increments and assigned as 28 February 2006, 18 March 2005, and 12 January 2004 (Figure 3, vertical lines). For shell $\delta^{18}\text{O}$, we assigned the calendar date to each isotope ratio and the Ba/Ca ratio.

To confirm the accuracy of daily growth increment counting, we counted the number of growth increments between the shell $\delta^{18}\text{O}$ maxima (Figure 3c). The number of days between the SST minimum and the next year SST minimum was 124 days during period A (15 June 2006 to 12 February 2006; Figure 3a), 343 days during period B (12 February 2006 to 7 March 2005; Figure 3b), and 428 days during period C (7 March 2005 to 5 January 2004; Figure 3c). The numbers of growth increments between the shell $\delta^{18}\text{O}$ maxima were 108 during period A, 348 during period B, and 432 during period C (Figure 3). When $\delta^{18}\text{O}_{\text{shell}}$ maxima correspond to the date of SST minima, the number of days and the number of growth increments coincide. The differences between the number of days and growth increments (day – increments) were 16 in period A, –5 in period B, and –4 in period C (Figure 3). Consequently, the number of increments between the shell $\delta^{18}\text{O}$ maxima almost corresponded with the number of days within increments counting error.

To validate the daily growth increment-based chronology, we established another chronology using the relationship between 16.6-day average SST and $\delta^{18}\text{O}_{\text{shell}}$. The resolution of the microsampling for $\delta^{18}\text{O}_{\text{shell}}$ analysis was approximately 400 μm , and there were 8 to 36 growth increments in the sampling grooves. On average, each $\delta^{18}\text{O}_{\text{shell}}$ datum reflected the 16.6-day average SST and $\delta^{18}\text{O}_{\text{sw}}$. We calculated the 16.6-day average SST from daily instrumental SST. The dates of the 16.6-day average SST minima in each year were 23 January 2006, 13 March 2005, and 7 January 2004, respectively. There was no significant difference in SST minima between the 1-day average SST and 16.6-day average SST except for 2006. As time control points, maxima of the $\delta^{18}\text{O}_{\text{shell}}$ were tied to the minima of the 16.6-day average SST. For 16.6-day average SST-based chronology, the dates and the number growth increments during each SST minima were as follows: From 15 June 2006 (collected date) to 23 January 2006 (143 days), the number of growth increments was 107. From 23 June 2006 to 13 March 2005 (315 days), the number of growth increments was 347. From 13 March 2005 to 7 January 2004 (432 days), the number of the growth increments was 431. Thus, using the 16.6-day average SST-based chronology, the differences between the number of days and the growth increments were 36, –32, and 1, respectively. We also compared daily SST running averages using weekly to monthly windows and found no significant differences. Therefore, the chronology based on daily growth increments was more accurate than the age model established from the chronology using SST and $\delta^{18}\text{O}_{\text{shell}}$.

These results showed that the growth increments in our specimen formed growth increments on a daily basis and confirmed the accuracy of a daily growth increment-based chronology. Thus, using giant clam daily growth increment-based chronology provides date to geochemical analysis if there are no enough resolution SST data available.

3.2. Stable Isotope Ratios in Okinotori *T. maxima*

The shell $\delta^{18}\text{O}$ ratios of the *T. maxima* shell ranged from -1.81 to -0.38‰ with an average of -1.25‰ ($n = 57$; Figure 3d). Lower $\delta^{18}\text{O}$ values in biogenic carbonates are normally associated with warmer and/or wetter conditions. The shell $\delta^{18}\text{O}$ ratios and SST were correlated with SST ($r = 0.62$, $p < 0.001$) from 21 November 2003 to 5 June 2006. The $\delta^{13}\text{C}$ ratios of the *T. maxima* shell ranged from 0.40 to 1.23 ‰ with an

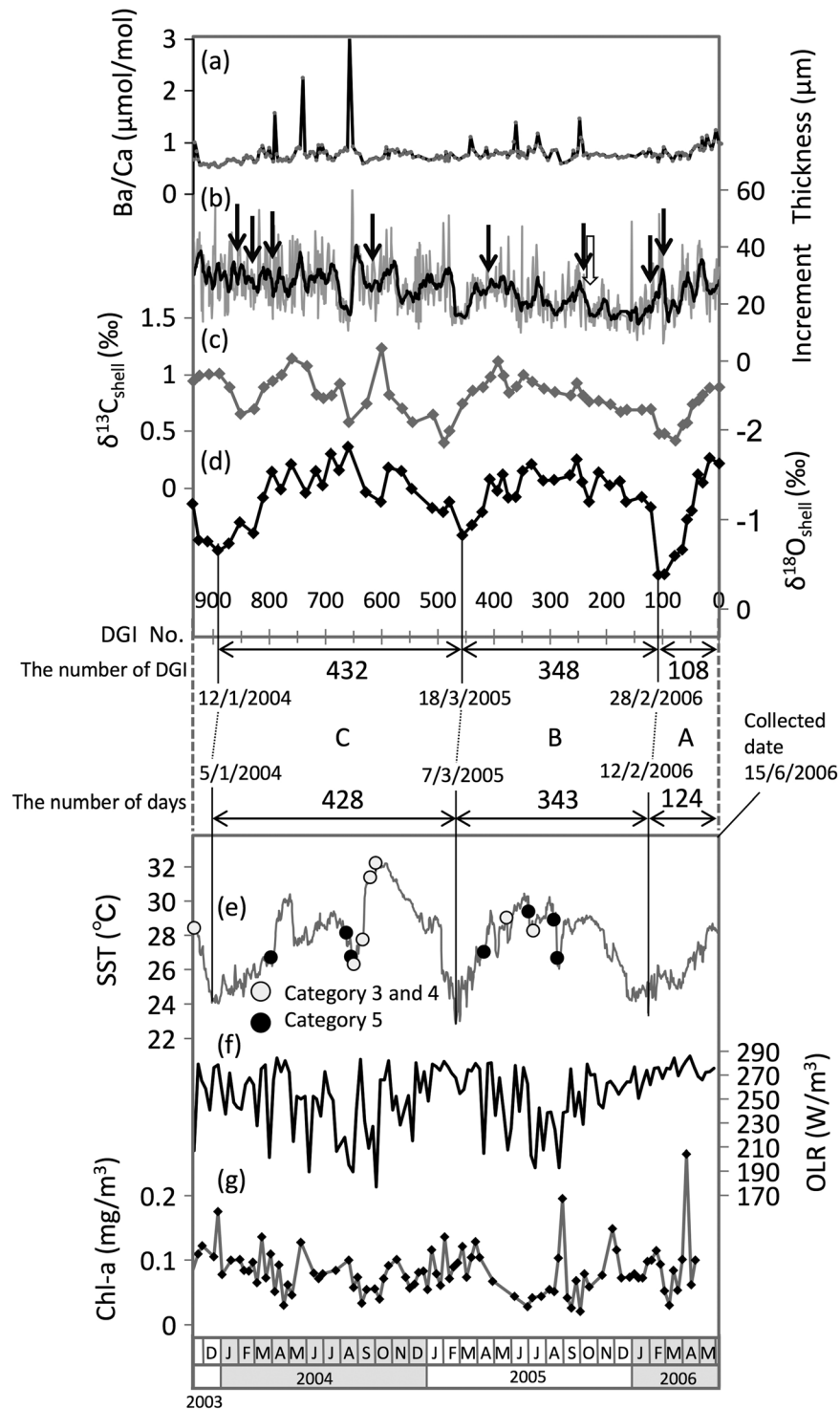


Figure 3. The time series of the geochemical and sclerochronological profiles in the *Tridacna maxima* shell and the environmental data of Okinotori Island. (a) Ba/Ca ratio in the shell, (b) growth increment thickness in the shell (thin line: row plots, solid line: 10-day average plots). The black and white arrows show growth breaks, and the white one is distinct growth break (see Figure 2), (c) carbon isotope ratio in the shell ($\delta^{13}\text{C}_{\text{shell}}$), and (d) oxygen isotope ratio in the shell ($\delta^{18}\text{O}_{\text{shell}}$). The $\delta^{18}\text{O}$ y axis is reversed for better comparison with the instrumental SST data. The numbers below the profile are the number of DGI (DGI: daily growth increments) between $\delta^{18}\text{O}_{\text{shell}}$ minima to the other minima. (e) Daily sea surface temperature (SST) from the observatory of Japan Agency for Marine-Earth Science and Technology. The numbers above the profile are the number of days between SST minima to the other minima. Category of the typhoons passing above Okinotori Island was shown as black circles (category 5: maximum wind speed larger than 33 m/s) and gray circles (category 3: maximum wind speed 18 to 24 m/s, category 4: maximum wind speed 25 to 32 m/s) above the SST profile. Maximum wind speed is 10-min average of wind speed, (f) weekly outgoing longwave radiation from satellite data of NOAA, and (g) Chl *a* concentration calculated from 8-day composite image of Sea-viewing Wide Field-of-view Sensor.

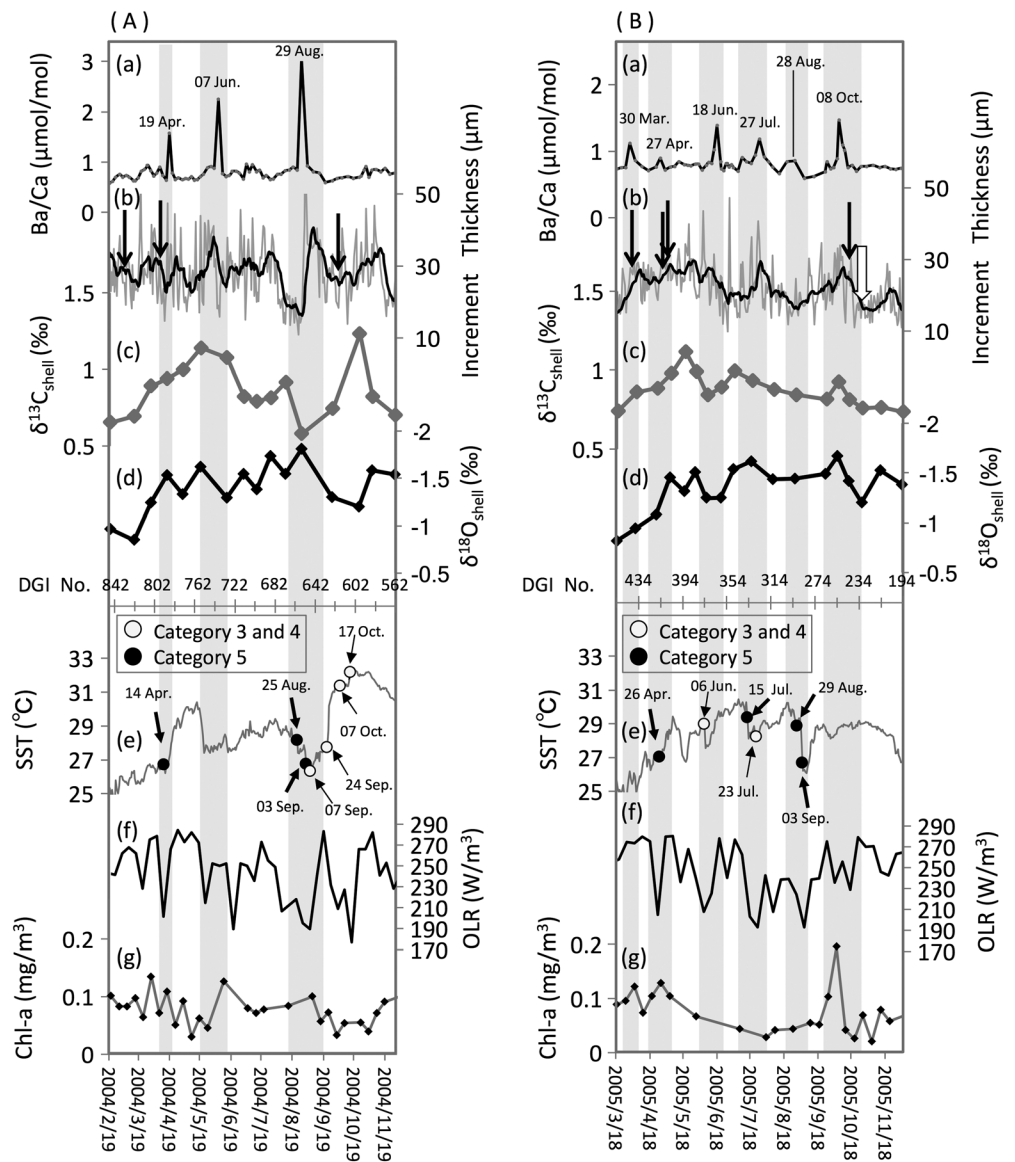


Figure 4. Enlarge images of typhoon periods described in Figure 3. (a) 2004 and (b) 2005 typhoon periods, respectively. (a) Ba/Ca ratio in the shell; the vertical lines show the Ba/Ca peaks. (b) Growth increment thickness in the shell (thin line: row plots, solid line: 10-day average plots). The black and white arrows show growth breaks, and the white one is distinct growth break (see Figure 2), (c) carbon isotope ratio in the shell ($\delta^{13}\text{C}_{\text{shell}}$), and (d) oxygen isotope ratio in the shell ($\delta^{18}\text{O}_{\text{shell}}$). The $\delta^{18}\text{O}$ y axis is reversed for better comparison with the instrumental SST data. (e) Daily sea surface temperature, (f) weekly outgoing longwave radiation from satellite data of NOAA, and (g) Chl *a* concentration calculated from 8-day composite image of Sea-viewing Wide Field-of-view Sensor.

average of 0.81‰ ($n = 57$; Figure 3c). The $\delta^{13}\text{C}$ ratios decreased during the period of lower SST (winter or typhoon season, e.g., 2004, 2005; Figures 3c and 3e).

3.3. Ba/Ca in Okinotori *T. maxima*

The Ba/Ca ratios of the *T. maxima* shell ranged from 0.53 to 3.06 μmol/mol, with an average of 0.79 μmol/mol ($n = 245$; Figure 3a). The Ba/Ca profile showed sharp positive peaks. The Ba/Ca peaks appeared (Figure 4, 2004: 19 April, 7 June, 29 August; 2005: 30 March, 27 April, 18 June, 27 July, and 8 October). The highest peak (3.07 μmol/mol) was in August–September 2004 when four typhoons passed across Okinotori Island in succession. However, there was also a Ba/Ca peak at 19 April and the end of March 2005, even though no typhoon approached (Figures 4a and 4e).

4. Discussion

4.1. Shell Growth Increments and Chronology

Comparison of SST records and $\delta^{18}\text{O}_{\text{shell}}$ confirms that the growth increments in *T. maxima* were daily growth increments and confirms the accuracy of the daily growth increment-based chronology. The two error factors for calendar date were uncertainty of the peak position of $\delta^{18}\text{O}_{\text{shell}}$ and formation of the growth increment. The difference in the chronology on a daily growth increment basis was large in period A. Since low SST continued in the winter of 2006, the date for the $\delta^{18}\text{O}_{\text{shell}}$ maximum may not coincide with the date of minimum water temperature. In addition, abrupt SST decreases on 12 February 2006 may have caused thermal stress to the specimen, and the specimen stopped or decreased growth, causing a growth break (14 February 2006; Figure 3b). The *T. maxima* specimen stopped growth and did not make a growth increment when the specimen was exposed to thermal stress. However, in periods B and C, the remainder (number of days – that of increments) showed more growth increments than the number of days between SST minima (5 and 4, respectively; Figure 3). These disagreements were within counting error ($\pm 1.3\%$ of increment number). Duprey et al. (2014) suggested that *T. maxima* sometimes made complex daily growth increments (subdaily growth increments) and it might be related to subdaily rhythms in shell deposition itself related to subdaily shell gaping behavior in *T. maxima*. Therefore, our specimen could also make complex growth increments and it might cause of over counting of growth increments. Although there was some uncertainty in of counting the growth increments, we could assign dates to geochemical analysis data using a daily growth increment-based chronology with 12.9%, 1.5%, and 0.9% counting error in periods A–C, respectively (Figure 3).

4.2. Shell Stable Oxygen Isotope Ratios

In this study, the $\delta^{18}\text{O}_{\text{sw}}$ in Okinotori Island is unknown; therefore, we assumed that $\delta^{18}\text{O}_{\text{sw}}$ was 0 ‰ and used the aragonitic shell bivalve relationship: $T(\text{ }^\circ\text{C}) = 21.8 - 4.69 * (\delta^{18}\text{O} - \delta^{18}\text{O}_{\text{sw}})$ (Grossman & Ku, 1986) for reconstruction of Okinotori Island SST. The instrumental SST and reconstructed SST differed. Causes of the differences are considered below.

First, insufficient sampling resolution of $\delta^{18}\text{O}_{\text{shell}}$ is a likely contributing factor. In March 2005, a reconstructed SST minimum (25.7 °C) was approximately 3 °C higher than the instrumental SST minimum (22.86 °C). In March 2005, the growth increment thickness suddenly fell below 20 μm for 26 days (23 February 2005 to 21 March 2005) with SST decrease (Figures 3b and 3e). The sampling point of maximum $\delta^{18}\text{O}_{\text{shell}}$ in 2005 included growth lines corresponding to 5 to 25 March 2005. The average instrumental SST from 5 to 25 March 2005 was 24.28 °C. Therefore, the disagreement between the reconstructed SST and instrumental SST in March 2005 was caused by a decreasing growth rate and reduction in the temporal resolution of $\delta^{18}\text{O}_{\text{shell}}$.

Second, the higher oxygen isotope ratios of seawater may cause the difference. The reconstructed SST minimum in February 2006 (23.6 °C) corresponded with the instrumental SST minimum in February 2006 (23.48 °C). However, from April to June 2006, the reconstructed SST was 1 °C higher than the instrumental SST. In this period, high OLR indicated that insolation promoted evaporation of seawater. The evaporation might lead to higher oxygen isotope ratios of seawater. Third, thermal stress to the giant clam might cause the differences. In January 2004, the reconstructed SST minimum (24.9 °C) almost corresponded with the instrumental SST minimum (24.11 °C). However, from October 2004 to February 2005, the reconstructed SST maximum (29.2 °C) was approximately 3 °C lower than the instrumental SST maximum (32.28 °C). After three typhoons from 25 August 2004 to 7 September 2004, the instrumental SST increased 6.06 °C during the period from 7 September 2004 to 20 October 2004. This SST increase (6.06 °C) was higher than the annual average SST amplitude (4.8 °C), and the SST reached 32.38 °C on 20 October 2004. In addition, the SST above 30 °C might stress the giant clam specimen (Andréfouët et al., 2013). Instrumental SST above 30 °C continued from 26 September 2004 to 16 December 2004. Indeed, the growth increment thickness fell below 30 μm from 16 November 2004 to 22 December 2004 (Figure 3b). The continuous high SST might hinder the growth of giant clam specimens. However, the decrease in growth caused by thermal stress was not a sufficient reason for the disagreement between the reconstructed SST and instrument SST at that time. The two $\delta^{18}\text{O}_{\text{shell}}$ values around November to December 2004 reflected SST from 2 to 13 November 2004 and from 17 November to 6 December

2004, respectively (Figures 3d and 3e). The average SST from 2 to 13 November 2004 was 31.89 °C, and the average SST from 17 November to 6 December 2004 was 30.77 °C. The disagreement between the reconstructed and instrumental SST in October 2004 was not completely explained by the reduction in the temporal resolution of $\delta^{18}\text{O}_{\text{shell}}$ with shell growth decrease.

Consequently, $\delta^{18}\text{O}_{\text{shell}}$ reflected annual SST fluctuation, while the reconstructed SST from $\delta^{18}\text{O}_{\text{shell}}$ is affected by the sampling resolution of the shell growth.

4.3. Synchronous Geochemical and Microstructural Signals in the Giant Clam Shell With Approaching Typhoons

The World Meteorological Organization categories of typhoons passing above Okinotori Island are shown as black circles (category 5: maximum wind speed above 33 m/s) and gray circles (category 3: maximum wind speed from 18 to 24 m/s; category 4: maximum wind speed from 25 to 32 m/s) above the SST profile (Figures 3 and 4). We distinguished the typhoons that affected the specimen habitat using the World Meteorological Organization category and whether the typhoons were within more than 500 km from Okinotori Island. We compared the time series of $\delta^{18}\text{O}_{\text{shell}}$, Ba/Ca, and increment thickness of the giant clam specimen to meteorological data (Figures 3 and 4). The shell Ba/Ca and $\delta^{18}\text{O}_{\text{shell}}$ profiles showed abrupt changes during periods of typhoons approach (Figures 3 and 4). In addition, there was a decrease in increment thickness and some disturbed growth increments after typhoon approach. The shell Ba/Ca and $\delta^{18}\text{O}_{\text{shell}}$ had positive peaks and decreasing increment thickness when SST suddenly decreased in May 2004.

4.3.1. Growth Increments and Growth Breaks

Hippopus hippopus (Tridacnidae; Linné, 1758) closes its valves and decreases its shell growth during an intense upwelling event (Aubert et al., 2009) and cyclone (Schwartzmann et al., 2011). In addition, Aubert et al. (2009) suggested that abrupt SST decrease caused a decrease in growth increment thickness. Our specimen (*T. maxima*) can also close its valves and decrease its shell growth when typhoon approaches. Indeed, there was a decrease in growth increment thickness during typhoon periods (Figures 3b and 4b). Cold upwelling water and strong waves caused by typhoons could stress the shell specimen. Shell growth quickly returned to normal after the typhoons (Figures 3b and 4b).

The specimen had nine growth breaks in its growth increments (see section 3.1). Previous studies revealed that the growth increment pattern of several bivalve species relates to environmental changes. For example, a growth break in hard-shell clams (*Mercenaria mercenaria*) is classified as a freeze-shock break, heat-shock break, thermal-shock break, abrasion break, spawning break, neap-tide break, or storm break via its micro-growth patterns (Kennish & Olsson, 1975). However, sclerochronology studies of giant clam are scarce (Aubert et al., 2009; Schwartzmann et al., 2011). Daily growth increments for giant clams would be a paleoenvironmental proxy with high temporal resolution. In our results, the *T. maxima* shell specimen had some growth breaks (arrows in Figures 2, 3b, and 4b). In particular, the distinct growth break around November 2005, characterized by a V-shape notch, was observed from the shell scute surface to the shell outer layer (white arrow in Figures 2d, 3c, and 4b). On 3 September 2005, the most powerful typhoon passed through the meteorological observation in Okinotori Island during 1993–2013. Another distinct break characterized by a notch in the shell outer layer corresponded to September 2004, when continuous typhoons passed the island (Figure 4e). These growth breaks suggest that typhoons can disturb the giant clam specimen habitat; simultaneously decreasing SST would be a stress for the specimen.

Not only environmental factors but also ontogenetic factors cause growth breaks. For instance, a spawning break could be a factor for growth breaks. Kubo and Iwai (2006) reported that *T. maxima* reaches sexual maturity at approximately 120 mm of shell length or 500,000-mm³ volume. Furthermore, *T. maxima* in Okinawa Island in southern Japan increases gonad development in spring (Kubo & Iwai, 2006). Although the timing of gonadal development of *T. maxima* in Okinotori Island is unknown, our *T. maxima* specimen shell length was 12.8 mm. Thus, the specimen likely reached sexual maturity, and reproduction may cause the growth breaks in the spring of each year (Figure 4b). It is possible to differentiate from its stratigraphic seasonality spring growth breaks (mainly seasonal spawning) and fall breaks (mainly typhoons) from its stratigraphic seasonality.

4.3.2. $\delta^{18}\text{O}_{\text{shell}}$ and SST Decrease With the Typhoon

The instrumental SST rapidly decreased after typhoons approached Okinotori Island (Figures 3e and 4e and Table 1). The base of Okinotori Island is a seamount from the deep sea (approximately 2,500 m) that causes

Table 1
The Instrumental and Reconstructed SST Changes During Typhoon Period and SST Decrease Period

Year	2004			2005	
	No typhoon	25 August and 3 and 7 September	6 June	15–23 July	29 August and 3 September
SST decrease periods (days)	20–24 May (5)	3 August to 7 September (35)	6 June to 16 July (11)	15–30 July (16)	1 September to 14 September (15)
Instrumental SST changes (°C)	2.45	3.09	1.3	2.17	3.08
Reconstructed SST period (days)	20 May to 15 June (26)	29 August to 29 September (31)	29 May to 8 June (10)	19 July to 8 August (20)	25 September to 28 October (33)
Reconstructed SST changes (°C)	1.5	2.8	1.2	0.8	2.2
$\delta^{18}\text{O}_{\text{shell}}$ changes (‰)	0.33	0.59	0.26	0.18	0.47

Note. Sea surface temperature (SST) decrease periods (days) indicate the SST decrease period due to the typhoons. Instrumental SST (°C) indicates the amplitude of instrumental SST changes during the typhoon period. Reconstructed SST periods (days) were decided using daily growth increment dating. Reconstructed SST (°C) and $\delta^{18}\text{O}_{\text{shell}}$ changes (‰) showed the amplitude of reconstructed SST and $\delta^{18}\text{O}_{\text{shell}}$ changes during the typhoon period, respectively.

upwelling (Genin & Boehlert, 1985). Heavy winds due to tropical cyclones also cause upwelling (Price, 1981). Consequently, typhoons approaching Okinotori Island cause upwelling and decreasing SST in the Okinotori Island reef. In addition, typhoon precipitation also causes decreased SST.

The $\delta^{18}\text{O}_{\text{shell}}$ reflected SST changes caused by typhoons (summary in Table 1).

For example, huge typhoons approached Okinotori Island on 29 August 2005 and especially 3 September 2005 (maximum wind speed 72 m/s; Figure 4e). The instrumental SST decreased 3.08 °C from 1 September 2005 (29.31 °C) to 7 September 2005 (after two typhoons, 26.23 °C), and the SST increased 2.56 °C to 15 September 2005 (28.79 °C; Figure 4e). The reconstructed SST from $\delta^{18}\text{O}_{\text{shell}}$ correspondingly decreased 2.2 °C at that time (Figure 4d).

There was a sharp decline in the SST with of 2.70 °C from 20 May 2004 (29.86 °C) to 24 May 2004 (27.41 °C) without typhoon (Figure 4e). The reconstructed SST from $\delta^{18}\text{O}_{\text{shell}}$ correspondingly decreased 1.5 °C at that time (Figure 4d).

The reconstructed SST changes were sometimes smaller than the instrumental SST changes when typhoons approached. On 15 July 2005 when the typhoon approached, the instrumental SST decreased 2.17 °C from 14 July (30.28 °C) to 16 July (28.11 °C; Figure 4e). However, the reconstructed SST from $\delta^{18}\text{O}_{\text{shell}}$ decreased 0.8 °C (Figure 4d). The OLR decreased when the typhoons approached, suggesting the development of cumulonimbus. The cumulonimbus caused precipitation, and $\delta^{18}\text{O}_{\text{sw}}$ decreased. Rainfall led to low $\delta^{18}\text{O}_{\text{shell}}$, and the reconstructed SST changes were consequently smaller than the instrumental SST changes, reflecting the combined effects of low $\delta^{18}\text{O}$ rainwater and high $\delta^{18}\text{O}_{\text{shell}}$ due to cooler SSTs. When typhoons approached Okinotori Island, as in September 2004 and September 2005, there were lags between the minima of the instrumental SST and the maxima for $\delta^{18}\text{O}_{\text{shell}}$ (Figures 4d and 4e and Table 1). These lags could result from the different geographical locations of the observatory and specimen. Because the location of the specimen was separated from the channel of the Okinotori Island reef, it might have delayed the SST decrease due to typhoons. Additionally, the insufficient sampling resolution could not reconstruct the minima of decreasing SST in the typhoon periods exactly.

Consequently, $\delta^{18}\text{O}_{\text{shell}}$ reflected SST decreases due to typhoons and the higher resolution $\delta^{18}\text{O}_{\text{shell}}$ may clearly reflect the SST changes caused by the typhoons.

4.3.3. Ba/Ca in *T. maxima*

Ba/Ca peaks in the *T. maxima* shell specimen appeared when a typhoon approached Okinotori Island (Figures 4a and 4e). Elliot et al. (2009) suggested that the amplitude and timing of Ba/Ca peaks in the inner layer of the *T. gigas* shell reflected the increase in chlorophyll concentration associated with phytoplankton blooms. Previous studies have suggested that Ba concentration in the bivalve shell reflects the concentration of dissolved or particulate Ba in ambient seawater (Lazareth et al., 2003; Vander Putten et al., 2000) and Ba-rich phytoplankton ingested by the shell specimen (Stecher et al., 1996). However, in the *Tridacna* shell, the exact mechanisms of Ba concentration in the shell have not been defined.

To investigate the mechanisms of Ba concentration in the *Tridacna* shell, we compare the Ba/Ca peaks and meteorological data. We compared the timing of the chlorophyll concentration near Okinotori Island with the Ba/Ca peaks in the shell specimen to estimate the effect of phytoplankton ingestion on the Ba/Ca peaks (Figure 4). The Ba/Ca peaks in the shell coincided with the chlorophyll peaks in April 2004, in June 2004, in September 2004, in March 2005, in April 2005, from September to November in 2005, and from April to May in 2006 (Figures 3a, 3g, 4a, and 4g). Yamazaki et al. (2011) reported that vertical mixing carried nutrients from deeper water to sea surface of Okinotori Island. Thus, the chlorophyll concentration increased during the period of the low SST and in typhoon seasons, which indicated the timing of vertical mixing and phytoplankton bloom. The Ba/Ca peaks in June 2004, March 2005, and October 2005 did not coincide with typhoons but corresponded with chlorophyll peaks and SST decreases (Figures 4a, 4e, and 4g). The period of the Ba/Ca peaks did not always correspond to chlorophyll peaks. The Ba/Ca peak in June 2005, July 2005, and August 2005 when the typhoons approached Okinotori Island did not coincide with chlorophyll concentration (Figures 4a and 4g). Chlorophyll data consisted of the 8-day average of the satellite observation, and thus, the amplitude and the timing of chlorophyll concentration might be underestimated because developed cumulonimbus estimated by low OLR values in these periods prevented satellite observation. In addition, shell Ba/Ca may be controlled not only by not ingestion of phytoplankton but also by variation in dissolved Ba in seawater. The vertical distribution of oceanic Ba is similar to that of nutrients (e.g., Lea et al., 1989; Monnin et al., 1999). Upwelling due to typhoons could bring Ba-rich deep-sea water to the surface of the Okinotori Island reef. Yamazaki et al. (2011) measured coral skeletal Ba/Ca in *Porites lobata* from Okinotori Island during the same period as this study, suggesting that coral Ba/Ca peaks and oceanic chlorophyll peaks appeared in typhoon season and winter with the supply of nitrate from deep-sea water. In addition, the coral Ba/Ca ranged from 5 to 14 $\mu\text{mol}/\text{mol}$ and averaged 6.6 $\mu\text{mol}/\text{mol}$ (Yamazaki et al., 2011), with different amplitude and values from the *T. maxima* shell Ba/Ca (0.53 to 3.06 $\mu\text{mol}/\text{mol}$, averaged 0.79 μmol) in this study. Because Ba in the coral skeleton reflects seawater-dissolved Ba, with a partition coefficient of $D_{\text{Ba}} = [\text{Ba}/\text{Ca}]_{\text{shell}}/[\text{Ba}/\text{Ca}]_{\text{water}} \approx 1$ (Alibert et al., 2003; Lea et al., 1989), D_{Ba} in *T. maxima* might be smaller than coral D_{Ba} . Comparing the Ba/Ca results in this study to those in Yamazaki et al. (2011), the *T. maxima* shell Ba/Ca peaks did not appear in winter (Figures 4a and S2 in the supporting information). The coral skeletal Ba/Ca peaks in winter were relatively smaller than the Ba/Ca peaks in the summer typhoon season. Thus, Ba/Ca peaks in winter did not appear in the *T. maxima* shell due to small D_{Ba} . However, Ba/Ca peaks in *T. maxima* clearly appeared in each typhoon period because the shell specimen had high temporal resolution records. Our sampling resolution (100- μm spot: 2 to 6 day) was sufficient to detect the typhoons. The range of shell Ba/Ca peaks suggested the influence of typhoons continued for 12.9 days (min. 8 days and max. 21 days; Figure 4). Ba/Ca peaks in the *T. maxima* specimen shell could be affected by the upwelling of Ba-rich seawater and its ingestion by phytoplankton, which bloomed due to this upwelling.

In summary, it is expected that the shell Ba/Ca peaks, the decrease in growth increment thickness, and the increase in oxygen isotope ratio of the *T. maxima* shell in Okinotori Island will occur as follows, regarding typhoons. During a typhoon, the giant clam closes its shell, the growth of the shell decreases, the growth increment thickness decreases, and sometimes, growth breaks with a sharp decrease in thickness appeared.

Okinotori Island is an atoll on the seamount, and thus, surface seawater was mixed with cold water from below the thermocline by the typhoon, and cold deep-sea water upwelled. As a result, cold deep-sea water increases $\delta^{18}\text{O}_{\text{shell}}$. Since deep-sea water has more Ba than surface seawater, Ba was captured from the surrounding seawater in the calcium carbonate of the shell, increasing Ba/Ca in the shell when shell growth recovered from typhoon stress. In addition, deep-sea water transported by upwelling due to a typhoon and vertical mixing in winter was abundant in nutrients, sometimes causing plankton blooms (chlorophyll concentration in seawater increases). The giant clam ingested these phytoplankton, and thus, significant Ba was taken up in the shell. Moreover, when the stress of environmental factors such as abrupt SST decreases and ecological stresses such as spawning time occur, the growth increment thickness decreases, and Ba/Ca peaks may occur.

5. Conclusions

We presented seasonal variations in $\delta^{18}\text{O}_{\text{shell}}$, $\delta^{13}\text{C}_{\text{shell}}$, Ba/Ca, and growth increment thicknesses in the *T. maxima* shell from Okinotori Island. By counting the daily growth increments in the shell, it is possible to

determine the exact date for geochemical analysis. In addition, $\delta^{18}\text{O}_{\text{shell}}$ reflected seasonal variations in SST. When typhoons approached Okinotori Island, the growth increment thickness decreased, $\delta^{18}\text{O}_{\text{shell}}$ increased, and the Ba/Ca showed positive peaks. The increment thickness of the *T. maxima* decreased with typhoon stress. Although similar patterns in growth and geochemistry occur in spring, these are attributed to spawning behavior that is restricted to spring, and the corresponding geochemical signals are restricted to the spring depositional layers that are distinct from the shell layers deposited from summer to fall typhoon season. By restricting our analysis to layers deposited during typhoon seasons, we avoid the potentially confounding influence of spawning signals by making use of the stratigraphic separation of the typhoon and spawning signals. An increase in $\delta^{18}\text{O}_{\text{shell}}$ during typhoons reflected a decrease in SST due to the typhoon. High resolution sampling for stable isotope analysis will improve the reconstruction of SST changes during typhoon periods. Positive peaks for Ba/Ca in the shell are considered to reflect upwelling and plankton blooms resulting from typhoons. Although the cause of the Ba/Ca peaks varies by region, these results suggest that by combining the growth increments and $\delta^{18}\text{O}_{\text{shell}}$, these signals will be a useful tool to reconstruct past typhoons using giant clam shell fossils.

Acknowledgments

Sampling of Okinotori giant clam occurred with the help of the crew on the R/V *Hakuhoumaru* KH-06-2. Sections of the shell specimen were prepared with the technical support of Tsuzumi Miyaji, Hidehiko Nomura, and Kousuke Nakamura. We acknowledge Tomohisa Irino for performing stable isotope measurement and Shirai laboratory members for conducting trace element analysis. The environmental data set was provided by Chika Sakata, M.S. 2006. This study was supported by JSPS KAKENHI grants JP 25257207, 15H03742 and 17H04708. All data available in the supporting information.

References

- Aharon, P. (1983). 140,000-yr isotope climatic record from raised coral reefs in New Guinea. *Nature*, *304*(5928), 720–723. <https://doi.org/10.1038/304720a0>
- Aharon, P. (1991). Recorders of reef environment histories: Stable isotopes in corals, giant clams, and calcareous algae. *Coral Reefs*, *10*(2), 71–90. <https://doi.org/10.1007/bf00571826>
- Aharon, P., & Chappell, J. (1986). Oxygen isotopes, sea level changes and the temperature history of a coral reef environment in New Guinea over the last 105 years. *Palaeogeography Palaeoclimatology Palaeoecology*, *56*(3–4), 337–379. [https://doi.org/10.1016/0031-0182\(86\)90101-X](https://doi.org/10.1016/0031-0182(86)90101-X)
- Alibert, C., Kinsley, L., Fallon, S. J., McCulloch, M. T., Berkelmans, R., & McAllister, F. (2003). Source of trace element variability in Great Barrier Reef corals affected by the Burdekin flood plumes. *Geochimica et Cosmochimica Acta*, *67*(2), 231–246. [https://doi.org/10.1016/S0016-7037\(02\)01055-4](https://doi.org/10.1016/S0016-7037(02)01055-4)
- Andréfouët, S., Van Wynsberge, S., Gaertner-Mazouni, N., Menkes, C., Gilbert, A., & Remoissenet, G. (2013). Climate variability and massive mortalities challenge giant clam conservation and management efforts in French Polynesia atolls. *Biological Conservation*, *160*, 190–199. <https://doi.org/10.1016/j.biocon.2013.01.017>
- Aubert, A., Lazareth, C., Cabioch, G., Boucher, H., Yamada, T., Iryu, Y., & Farman, R. (2009). The tropical giant clam *Hippopus hippopus* shell, a new archive of environmental conditions as revealed by sclerochronological and $\delta^{18}\text{O}$ profiles. *Coral Reefs*, *28*(4), 989–998. <https://doi.org/10.1007/s00338-009-0538-0>
- Ayling, B. F., Chappell, J., Gagan, M. K., & McCulloch, M. T. (2015). ENSO variability during MIS 11 (424–374 ka) from *Tridacna gigas* at Huon Peninsula, Papua New Guinea. *Earth and Planetary Science Letters*, *431*, 236–246. <https://doi.org/10.1016/j.epsl.2015.09.037>
- Bonham, K. (1965). Growth rate of giant clam *Tridacna gigas* at bikini atoll as revealed by radioautography. *Science New Series*, *149*(3681), 300–302.
- Duprey, N., Lazareth, C. E., Dupouy, C., Butscher, J., Farman, R., Maes, C., & Cabioch, G. (2014). Calibration of seawater temperature and $\delta^{18}\text{O}$ seawater signals in *Tridacna maxima*'s $\delta^{18}\text{O}_{\text{shell}}$ record based on in situ data. *Coral Reefs*, *34*(2), 437–450. <https://doi.org/10.1007/s00338-014-1245-z>
- Elliot, M., Welsh, K., Chilcott, C., McCulloch, M., Chappell, J., & Ayling, B. (2009). Profiles of trace elements and stable isotopes derived from giant long-lived *Tridacna gigas* bivalves: Potential applications in paleoclimate studies. *Palaeogeography Palaeoclimatology Palaeoecology*, *280*(1–2), 132–142. <https://doi.org/10.1016/j.palaeo.2009.06.007>
- Epstein, S., Buchsbaum, R., Lowenstam, H. A., & Urey, H. C. (1953). Revised carbonate-water isotopic temperature scale. *Geological Society of America Bulletin*, *64*(11), 1315–1325. [https://doi.org/10.1130/0016-7606\(1953\)64](https://doi.org/10.1130/0016-7606(1953)64)
- Fan, D., & Liu, K. (2008). Perspectives on the linkage between typhoon activity and global warming from recent research advances in paleotempestology. *Chinese Science Bulletin*, *53*(19), 2907–2922.
- Faylona, M. G. P. G., Lazareth, C. E., Sémah, A.-M., Caquineau, S., Boucher, H., & Ronquillo, W. P. (2011). Preliminary study on the preservation of giant clam (*Tridacnidae*) shells from the Balobok Rockshelter archaeological site, south Philippines. *Geoarchaeology*, *26*(6), 888–901. <https://doi.org/10.1002/gea.20377>
- Forsyth, A. J., Nott, J., & Bateman, M. D. (2010). Beach ridge plain evidence of a variable late-Holocene tropical cyclone climate, North Queensland, Australia. *Palaeogeography Palaeoclimatology Palaeoecology*, *297*(3–4), 707–716. <https://doi.org/10.1016/j.palaeo.2010.09.024>
- Frapppier, A. B. (2008). A stepwise screening system to select storm-sensitive stalagmites: Taking a targeted approach to speleothem sampling methodology. *Quaternary International*, *187*(1), 25–39. <https://doi.org/10.1016/j.quaint.2007.09.042>
- Genin, A., & Boehlert, G. W. (1985). Dynamics of temperature and chlorophyll structures above a seamount: An oceanic experiment. *Journal of Marine Research*, *43*(4), 907–924. <https://doi.org/10.1357/002224085788453868>
- Gillikin, D. P., Dehairs, F., Lorrain, A., Steenmans, D., Baeyens, W., & André, L. (2006). Barium uptake into the shells of the common mussel (*Mytilus edulis*) and the potential for estuarine paleo-chemistry reconstruction. *Geochimica et Cosmochimica Acta*, *70*(2), 395–407. <https://doi.org/10.1016/j.gca.2005.09.015>
- Goodwin, D. H., Schöne, B. R., Dettman, D. L., Goodwin, D. H., & Scho, B. R. (2003). Resolution and fidelity of oxygen isotopes as paleotemperature proxies in bivalve mollusk shells: Models and observations. *Palaio*, *18*(2), 110–125.
- Grossman, E. L., & Ku, T. L. (1986). Oxygen and carbon isotope fractionation in biogenic aragonite: Temperature effects. *Chemical Geology*, *59*, 59–74. [https://doi.org/10.1016/0168-9622\(86\)90057-6](https://doi.org/10.1016/0168-9622(86)90057-6)
- Haig, J., Nott, J., & Reichert, G.-J. (2014). Australian tropical cyclone activity lower than at any time over the past 550–1,500 years. *Nature*, *505*(7485), 667–671. <https://doi.org/10.1038/nature12882>

- Hetzinger, S., Pfeiffer, M., Dullo, W. C., Keenlyside, N., Latif, M., & Zinke, J. (2008). Caribbean coral tracks Atlantic Multidecadal Oscillation and past hurricane activity. *Geology*, *36*(1), 11–14. <https://doi.org/10.1130/G24321A.1>
- Horibe, Y., & Oba, T. (1972). Temperature scales of aragonite-water and calcite-water system. *Fossils*, *23*(24), 69–79.
- Horton, B. P., Rossi, V., & Hawkes, A. D. (2009). The sedimentary record of the 2005 hurricane season from the Mississippi and Alabama coastlines. *Quaternary International*, *195*(1–2), 15–30. <https://doi.org/10.1016/j.quaint.2008.03.004>
- IPCC (2013). In T. F. Stocker, et al. (Eds.), *Climate Change 2013: The Physical Science Basis. Contribution of Working Group I to the Fifth Assessment Report of the Intergovernmental Panel on Climate Change* (Ch. SPM, pp. 1–30). Cambridge University Press.
- Iwao, N., Junichi, K., Hidetoshi, F., & Hirohumi and Hirohumi, Y. (2002). Marine weather observation at Oki-no-tori sima. *Meteorological Society of Japan*, *49*(7), 569–579.
- Jones, D. S., Williams, D. F., & Romanek, C. S. (1986). Life history of symbiont-bearing giant clams from stable isotope profiles. *Science*, *231*(4733), 46–48.
- Kennish, M. J., & Olsson, R. K. (1975). Effect of thermal discharges on the microstructural growth of *Mercenaria mercenaria*. *Environmental Geology*, *1*(1), 41–64. <https://doi.org/10.1007/BF02426940>
- Kilbourne, K. H., Moyer, R. P., Quinn, T. M., & Grotoli, A. G. (2011). Testing coral-based tropical cyclone reconstructions: An example from Puerto Rico. *Palaeogeography Palaeoclimatology Palaeoecology*, *307*(1–4), 90–97. <https://doi.org/10.1016/j.palaeo.2011.04.027>
- Knapp, P. A., Maxwell, J. T., & Soule, P. T. (2016). Tropical cyclone rainfall variability in coastal North Carolina derived from longleaf pine (*Pinus palustris* mill.): AD 1771–2014. *Climatic Change*, *135*(2), 311–323. <https://doi.org/10.1007/s10584-015-1560-6>
- Komagoe, T., Watanabe, T., Shirai, K., Yamazaki, A., & Uemasu, M. (2016). High temporal resolution analysis for palaeo environments using giant clam shells: Elongate giant clam *Tridacna maxima* shell reveals typhoon events Okinotori Island, Japan, *Kaiyo extra*, *56*, 80–93.
- Kubo, H., & Iwai, K. (2006). Seasonal fluctuation on gonadal maturation of *Tridacna maxima*. *Annual Report of Okinawa Fishery and Ocean Research Center*, *68*, 211–214.
- Lane, C. S., Hildebrandt, B., Kennedy, L. M., LeBlanc, A., Liu, K.-B., Wagner, A. J., & Hawkes, A. D. (2017). Verification of tropical cyclone deposits with oxygen isotope analyses of coeval ostracod valves. *Journal of Paleolimnology*, *57*(3), 245–255. <https://doi.org/10.1007/s10933-017-9943-5>
- Lawrence, J. R., Hyeong, K., Maddocks, R. F., & Lee, K.-S. (2008). Passage of tropical storm Allison (2001) over southeast Texas recorded in $\delta^{18}\text{O}$ values of *Ostracoda*. *Quaternary Research*, *70*(02), 339–342. <https://doi.org/10.1016/j.yqres.2008.04.004>
- Lazareth, C. E., Vander Putten, E., André, L., & Dehairs, F. (2003). High-resolution trace element profiles in shells of the mangrove bivalve *Isognomon ephippium*: A record of environmental spatio-temporal variations? *Estuarine, Coastal and Shelf Science*, *57*(5–6), 1103–1114. [https://doi.org/10.1016/S0272-7714\(03\)00013-1](https://doi.org/10.1016/S0272-7714(03)00013-1)
- Lea, D. W., Shen, G. T., & Boyle, E. A. (1989). Coralline barium records temporal variability in equatorial Pacific upwelling. *Nature*, *340*(6232), 373–376. <https://doi.org/10.1038/340373a0>
- Li, Z. H., Labbé, N., Driese, S. G., & Grissino-Mayer, H. D. (2011). Micro-scale analysis of tree-ring $\delta^{18}\text{O}$ and $\delta^{13}\text{C}$ on α -cellulose spline reveals high-resolution intra-annual climate variability and tropical cyclone activity. *Chemical Geology*, *284*(1–2), 138–147. <https://doi.org/10.1016/j.chemgeo.2011.02.015>
- McClain, C. R., Feldman, G. C., & Hooker, S. B. (2004). An overview of the SeaWiFS project and strategies for producing a climate research quality global ocean bio-optical time series. *Deep Sea Research Part II: Topical Studies in Oceanography*, *51*(1–3), 5–42. <https://doi.org/10.1016/j.dsr2.2003.11.001>
- Miller, D. L., Mora, C. I., Grissino-Mayer, H. D., Mock, C. J., Uhle, M. E., & Sharp, Z. (2006). Tree-ring isotope records of tropical cyclone activity. *Proceedings of the National Academy of Sciences of the United States of America*, *103*(39), 14,294–14,297. <https://doi.org/10.1073/pnas.0606549103>
- Moir, B. G. (1986). A review of tridacnid ecology and some possible implications for archaeological research. *Asian Perspectives*, *27*(1), 95–121.
- Monnin, C., Jeandel, C., Cattaldo, T., & Dehairs, F. (1999). The marine barite saturation state of the world's oceans. *Marine Chemistry*, *65*, 253–261.
- Muller, J., Collins, J. M., Gibson, S., & Paxton, L. (2017). Recent Advances in the Emerging Field of Paleotempestology. In *Hurricanes and Climate Change* (pp. 1–33). Springer International Publishing, Cham.
- Nakano, I., Fujimori, H., & Kimura, J. (2001). Marine weather observation at Oki-no-tori sima. *JAMSTECR*, *43*, 143–152.
- Nott, J. (2011). A 6000 year tropical cyclone record from Western Australia. *Quaternary Science Reviews*, *30*(5–6), 713–722. <https://doi.org/10.1016/j.quascirev.2010.12.004>
- Nott, J., & Forsyth, A. (2012). Punctuated global tropical cyclone activity over the past 5,000 years. *Geophysical Research Letters*, *39*, L14703. <https://doi.org/10.1029/2012GL052236>
- Nott, J., Smithers, S., Walsh, K., & Rhodes, E. (2009). Sand beach ridges record 6000 year history of extreme tropical cyclone activity in northeastern Australia. *Quaternary Science Reviews*, *28*(15–16), 1511–1520. <https://doi.org/10.1016/j.quascirev.2009.02.014>
- Pannella, G., & MacClintock, C. (1968). Biological and environmental rhythms reflected in molluscan shell growth. In D. B. Macurda Jr. (Ed.), *Paleobiological Aspects of Growth and Development: A Symposium vol. 2. Paleontological Society Memoir* (pp. 64–80).
- Pätzold, J., Heinrichs, J., Wolschendorf, K., & Wefer, G. (1991). Correlation of stable oxygen isotope temperature record with light attenuation profiles in reef-dwelling *Tridacna* shells. *Coral Reefs*, *10*(2), 65–69. <https://doi.org/10.1007/bf00571825>
- Price, J. F. (1981). Upper Ocean response to a hurricane. *Journal of Physical Oceanography*, *11*(2), 153–175. [https://doi.org/10.1175/1520-0485\(1981\)011%3C0153:UORTAH%3E2.0.CO;2](https://doi.org/10.1175/1520-0485(1981)011%3C0153:UORTAH%3E2.0.CO;2)
- Romanek, C. S., & Grossman, E. L. (1989). Stable isotope profiles of *Tridacna maxima* as environmental indicators. *Palaios*, *4*(5), 402–413.
- Rosewater, J. (1965). The family Tridacnidae in the Indo-Pacific. *Indo-Pacific Mollusca*, *1*, 347–396.
- Sano, Y., Kobayashi, S., Shirai, K., Takahata, N., Matsumoto, K., Watanabe, T., et al. (2012). Past daily light cycle recorded in the strontium/calcium ratios of giant clam shells. *Nature Communications*, *3*(1), 761. <https://doi.org/10.1038/ncomms1763>
- Schone, B. R., Dunca, E., Fiebig, J., & Pfeiffer, M. (2005). Mutvei's solution: An ideal agent for resolving microgrowth structures of biogenic carbonates. *Palaeogeography Palaeoclimatology Palaeoecology*, *228*(1–2), 149–166. <https://doi.org/10.1016/j.palaeo.2005.03.054>
- Schwartzmann, C., Durrieu, G., Sow, M., Ciret, P., Lazareth, C. E., & Massabuau, J.-C. (2011). In situ giant clam growth rate behavior in relation to temperature: A one-year coupled study of high-frequency noninvasive valvometry and sclerochronology. *Limnology and Oceanography*, *56*(5), 1940–1951. <https://doi.org/10.4319/lo.2011.56.5.1940>
- Shirai, K., Kawashima, T., Sowa, K., Watanabe, T., Nakaniori, T., Takahata, N., et al. (2008). Minor and trace element incorporation into branching coral *Acropora nobilis* skeleton. *Geochimica et Cosmochimica Acta*, *72*(22), 5386–5400. <https://doi.org/10.1016/j.gca.2008.07.026>
- Shupe, M. D., & Intrieri, J. M. (2004). Cloud radiative forcing of the Arctic surface: The influence of cloud properties, surface albedo, and solar zenith angle. *Journal of Climate*, *17*(3), 616–628. [https://doi.org/10.1175/1520-0442\(2004\)017%3C0616:RFOTA%3E2.0.CO;2](https://doi.org/10.1175/1520-0442(2004)017%3C0616:RFOTA%3E2.0.CO;2)

- Stecher, H. A., Krantz, D. E., Lord, C. J., Luther, G. W., & Bock, K. W. (1996). Profiles of strontium and barium in *Mercenaria mercenaria* and *Spisula solidissima* shells. *Geochimica et Cosmochimica Acta*, 60(18), 3445–3456. [https://doi.org/10.1016/0016-7037\(96\)00179-2](https://doi.org/10.1016/0016-7037(96)00179-2)
- Trouet, V., Harley, G. L., & Domínguez-Delmás, M. (2016). Shipwreck rates reveal Caribbean tropical cyclone response to past radiative forcing. *Proceedings of the National Academy of Sciences of the United States of America*, 113(12), 3169–3174. <https://doi.org/10.1073/pnas.1519566113>
- Urey, H. C., Lowenstam, H. A., Epstein, S., & McKinney, C. R. (1951). Measurement of paleotemperatures and temperatures and the southeastern United States. *Bulletin Geological Society of America*, 62, 399–416. [https://doi.org/10.1130/0016-7606\(1951\)62%5B399:MOPATO%5D2.0.CO;2](https://doi.org/10.1130/0016-7606(1951)62%5B399:MOPATO%5D2.0.CO;2)
- Vander Putten, E., Dehairs, F., Keppens, E., & Baeyens, W. (2000). High resolution distribution of trace elements in the calcite shell layer of modern *Mytilus edulis*: Environmental and biological controls. *Geochimica et Cosmochimica Acta*, 64(6), 997–1011. [https://doi.org/10.1016/S0016-7037\(99\)00380-4](https://doi.org/10.1016/S0016-7037(99)00380-4)
- Warter, V., & Müller, W. (2017). Daily growth and tidal rhythms in Miocene and modern giant clams revealed via ultra-high resolution LA-ICPMS analysis—A novel methodological approach towards improved sclerochemistry. *Palaeogeography Palaeoclimatology Palaeoecology*, 465, 362–375. <https://doi.org/10.1016/j.palaeo.2016.03.019>
- Warter, V., Muller, W., Wesselingh, F. P., Todd, J. A., & Renema, W. (2015). Late miocene seasonal to subdecadal climate variability in the indo-west pacific (East Kalimantan, Indonesia) preserved in giant clams. *Palaeos*, 30(1), 66–82. <https://doi.org/10.2110/palo.2013.061>
- Watanabe, T., & Oba, T. (1999). Daily reconstruction of water temperature from oxygen isotopic ratios of a modern *Tridacna* shell using a freezing microtome sampling technique. *Journal of Geophysical Research*, 104(C9), 20,667–20,674. <https://doi.org/10.1029/1999JC900097>
- Watanabe, T., Suzuki, A., Kawahata, H., Kan, H., & Ogawa, S. (2004). A 60-year isotopic record from a mid-Holocene fossil giant clam (*Tridacna gigas*) in the Ryukyu Islands: Physiological and paleoclimatic implications. *Palaeogeography Palaeoclimatology Palaeoecology*, 212(3–4), 343–354. <https://doi.org/10.1016/j.palaeo.2004.07.001>
- Williams, H. F. L. (2012). Magnitude of Hurricane Ike storm surge sedimentation: Implications for coastal marsh aggradation. *Earth Surface Processes and Landforms*, 37(8), 901–906. <https://doi.org/10.1002/esp.3252>
- Woodruff, J. D., Donnelly, J. P., & Okusu, A. (2009). Exploring typhoon variability over the mid-to-late Holocene: Evidence of extreme coastal flooding from Kamikoshiki, Japan. *Quaternary Science Reviews*, 28(17–18), 1774–1785. <https://doi.org/10.1016/j.quascirev.2009.02.005>
- Yamazaki, A., Watanabe, T., Ogawa, N. O., Ohkouchi, N., Shirai, K., Toratani, M., & Uematsu, M. (2011). Seasonal variations in the nitrogen isotope composition of Okinotori coral in the tropical western Pacific: A new proxy for marine nitrate dynamics. *Journal of Geophysical Research*, 116, G04005. <https://doi.org/10.1029/2011JG001697>
- Yoneyama, S., Seno, K., Maeda, H., Okada, A., & Hayashibara, T. (2006). Marine animals on the coral reefs of Okino-torishima. *Tokyo Metropolitan Research on Fisheries Science*, 1, 73–85.

Erratum

In the originally published version of this paper, the funding source, JSPS KAKENHI, was incorrectly spelled and grant JP 17H04708 was omitted in the Acknowledgments section. This error has since been corrected, and this version can be considered the authoritative version.